Measuring Relative Grain-Boundary Energies in Block-Copolymer Microstructures

Hyung Ju Ryu, David B. Fortner, Gregory S. Rohrer, and Michael R. Bockstaller*

Department of Materials Science and Engineering, Carnegie Mellon University, 5000 Forbes Avenue, Pittsburgh, Pennsylvania 15213, USA

(Received 15 November 2011; published 6 March 2012)

The (relative) energies of symmetric tilt grain boundaries in a strongly segregated lamellar block copolymer are determined by analysis of the dihedral angles at grain-boundary triple junctions. The analysis reveals two regimes: at low and intermediate misorientations (corresponding to a tilt-angle range $0 \leq \theta \leq 85°$) the grain-boundary energy is found to depend on the tilt angle as $E(\theta) \sim \theta^x$, with $2.5 > x \geq 0$. At large misorientations the grain-boundary energy is found to be independent (within the experimental uncertainty) of the angle of tilt. The transition between the two scaling regimes is accompanied by the transition of the grain-boundary structure from the chevron to the omega morphology. Grain-boundary energy and frequency are found to be inversely related, thus suggesting boundary energy to be an important parameter during grain coarsening in block-copolymer microstructures, as it is in inorganic polycrystalline microstructures.

DOI: 10.1103/PhysRevLett.108.107801 PACS numbers: 61.30.Jf, 61.41.+e, 68.55.am, 81.30.Hd

The ability to self-organize into periodically ordered microdomain morphologies makes block-copolymer-based materials intriguing platforms to facilitate transformative technological breakthroughs in a range of areas, including dynamic photonic sensors, solid state ion conductors, and bulk heterojunction materials for polymer photovoltaics [1–5]. In these applications, nonequilibrium structural defects such as grain boundaries (GB) are expected to play an important role in determining material performance because of their impact on the long-range order and tortuosity of diffusion pathways. The occurrence of GB defects is inherent in quiescent organized block-copolymer (BCP) microstructures and can be related to the nucleation and growth of ordered grains during the structure evolution process, the interaction of disclinations, or mechanically induced kinking because of inhomogeneous solvent evaporation during the late stages of film formation. The basic phenomenology of GB structures in BCP materials was first discussed by Gido and Thomas who classified and evaluated the various GB types associated with tilt and twist deformations of lamellar BCPs [6–9]. Subsequent experimental studies revealed the relevance of process parameters (such as the application of shear fields), molecular architecture, and composition on GB formation as well as the implications of GB defects on, for example, the permeability of BCP materials [10–17].

Despite the abundance of GB defects and their demonstrated relevance on the physical properties of BCP materials, very little is known about the governing parameters that determine the formation of the various types of GB structures in BCPs or the evolution of GB structures during, for example, thermal annealing. One parameter that is of particular interest is the energy penalty associated with GB formation as it provides insight into both the mechanism and driving force of grain coarsening during annealing. The current understanding of GB energies in BCPs is limited to simulation studies, for example, by Schick and co-workers as well as Matsen who—using a Ginzburg-Landau free-energy and self-consistent field approach, respectively—evaluated the surface energy of various types of tilt GB structures in weakly segregated lamellar BCP [18–20]. While these studies have established the principal trends of the GB energy for various GB types and also provided a rationale for experimental observations such as the transition from chevron- to Ω-type morphologies with increasing misorientation of symmetric tilt GBs, a more quantitative understanding of the structure evolution in BCP systems will require the experimental determination of GB energies. The purpose of this Letter is to present an experimental methodology to determine the (relative) energies of GBs in BCP materials based on the analysis of dihedral angles at triple-junction lines. We find that the energy of symmetric tilt GBs in a strongly segregated lamellar BCP approximately follows the predicted trend with tilt angle θ and we demonstrate that the frequency of symmetric tilt GBs in annealed BCPs is inversely related to the GB energy. While the GB energy exhibits similar scaling regimes as predicted by simulation, the transition between the scaling regimes is found to be shifted to smaller tilt angles along with the reduction of the threshold angle for the chevron $\rightarrow \Omega$ transition. With appropriately large data sets, the technique is expected to be equally applicable to determine the relative energies of asymmetric tilt or twist GB structures as well as GB energies in arbitrary BCP microdomain morphologies.

Figure 1(a) illustrates the relevant geometrical parameters of a triple-junction line **l** that is formed by the intersection of three GBs [21,22]. Under the assumption of local equilibrium the geometry of a triple junction results as a consequence of mechanical equilibrium between the boundaries that is described by Herring's equation [23]

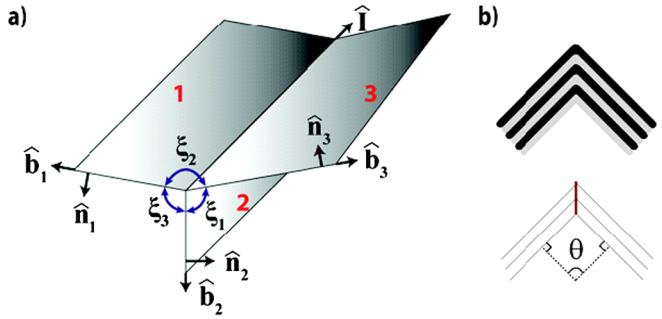

FIG. 1 (color online). (a) Illustration of triple-junction geometry. ξ_i denotes the dihedral angles, $\mathbf{l}$ the triple-junction line, $\mathbf{b}$ is the boundary tangent, and $\mathbf{n}$ is the boundary normal. (b) Illustration of symmetric tilt grain boundary in lamellar system. The boundary (indicated as bold) bisects the tilt angle θ.

$$\sum_{i=1}^{3}\left[\sigma_i b_i + \left(\frac{\partial \sigma_i}{\partial \varphi_i}\right) n_i\right] = \mathbf{0}. \tag{1}$$

Here $\sigma_i = (\partial E_i/\partial A)$ is the surface tension of the ith GB, $\mathbf{n}_i$ is the unit normal of the ith GB, and $\mathbf{b}_i$ is a unit vector that lies within the ith GB and is normal to the triple-junction line $\mathbf{l}$. The angle φ_i is defined as the right-handed angle of rotation of the ith boundary about $\mathbf{l}$. The first term in Eq. (1) describes the force balance of the intersecting GB while the second term presents the torque necessary to rotate the boundary into the equilibrium position.

If the GB energy is assumed to be independent of the GB plane orientation, Eq. (1) reduces to Young's equation [24]. The latter yields (for each triple junction) a set of two independent equations that relate the three unknown GB energies σ_i with their respective dihedral (or contact) angle ξ_i opposite to the boundary:

$$\frac{\sigma_1}{\sin\xi_1} = \frac{\sigma_2}{\sin\xi_2} = \frac{\sigma_3}{\sin\xi_3}. \tag{2}$$

From the evaluation of a sufficiently large number of triple junctions, the GB energies can then be determined using a statistical method that has been described in detail in Ref. [25]. The procedure can be summarized as follows. In a first step, the range of misorientation (for the case of symmetric tilt GBs the misorientation is equal to the tilt angle between adjacent grains) is discretized into n subintervals of width π/n. Subsequently, the set of dihedral angles obtained from the analysis of triple junctions is binned corresponding to the tilt angle of the respective GBs to obtain a set of $n(n-1)/2$ averaged equations of the form $\sum_{j=1}^{n} A_{ij}\sigma_j = g_i$ [with $i = 1, 2, \ldots, n(n-1)/2$ and $j = 1, 2, \ldots, n$], where A_{ij} is the matrix of coefficients corresponding to the averaged values of energy, $\langle\sigma_j\rangle$ is the set of average GB energies that is to be determined, and g_i is the null vector. The resulting set of equations (in which $\langle\boldsymbol{\sigma}\rangle$ is overdetermined) can be solved efficiently using the Kaczmarz iteration method [25]. It should be mentioned that, for the procedure described above to be accurate, sufficient sampling of triple junctions is required. The approximate error associated with the numerical procedure used to determine $\langle\boldsymbol{\sigma}\rangle$ can be estimated by random subdivision of the set of triple junctions into groups and subsequent comparison of the results of $\langle\boldsymbol{\sigma}\rangle$ for each group. The triple-junction method has been successfully applied to determine the relative GB energies in metal and ceramic structures and it will be used in the following to determine the surface tension of symmetric tilt GBs in lamellar BCP systems [26]. Figure 1(b) illustrates a symmetric tilt GB in a layered (BCP) structure—the boundary (indicated as a bold line) symmetrically bisects the rotation angle θ about an axis within the boundary plane. Symmetric tilt GB structures present an ideal model system to demonstrate the application of the triple-junction technique because of their relative abundance in BCP microdomain structures as well as the extensive amount of theoretical work on this particular type of GB that provides a context for the discussion of our results.

The material system in our study consists of a near-symmetric poly(styrene-*b*-isoprene) (PS-PI) copolymer with molecular weight $M_w = 79.6$ kg/mol, a molecular weight dispersity index $M_w/M_n = 1.05$, and a volume fraction of styrene component of $\phi_{\mathrm{PS}} = 0.48$. With $\chi N \cong 94$ (where $\chi = 0.08$ denotes the Flory interaction parameter and N the degree of polymerization), the PS-PI copolymer is about in the strong segregation regime. Films of 1 mm thickness were cast under rapid solvent evaporation conditions ($T = 23\,^{\circ}\mathrm{C}$, partial pressure of toluene $p = 80$ mbar) from 5% (by weight) toluene solution to provide for high GB densities during film formation. Samples were subsequently thermally annealed in vacuum at $T = 120\,^{\circ}\mathrm{C}$ for 72 and 166 h, respectively, to achieve local equilibrium at triple junctions [27]. Two distinct annealing times were chosen to assess whether local equilibrium was established. Grain-boundary types and triple junctions were identified using TEM on 412 $\mu\mathrm{m}^2$ (505 $\mu\mathrm{m}^2$) sample areas for a specimen after 72 h (166 h) of thermal annealing. To identify the grain structure of the BCP, series of micrographs were successively processed by skeletonization, discretization, and Fourier transform to determine the grain misorientation with regard to a laboratory reference frame that is defined by the film casting geometry [28]. We note that for the purpose of the present discussion of GB energies, the details regarding the laboratory reference frame are of no relevance. A comprehensive presentation of the image analysis procedure and the significance of the reference frame will be provided in a future publication. Figure 2(a) illustrates the grain map that was obtained by image analysis of a representative electron micrograph. The figure reveals several triple junctions that are formed by the intersection of GBs. Grain boundaries with less than 5° twist contribution and with a disorientation of less than 10° between boundary

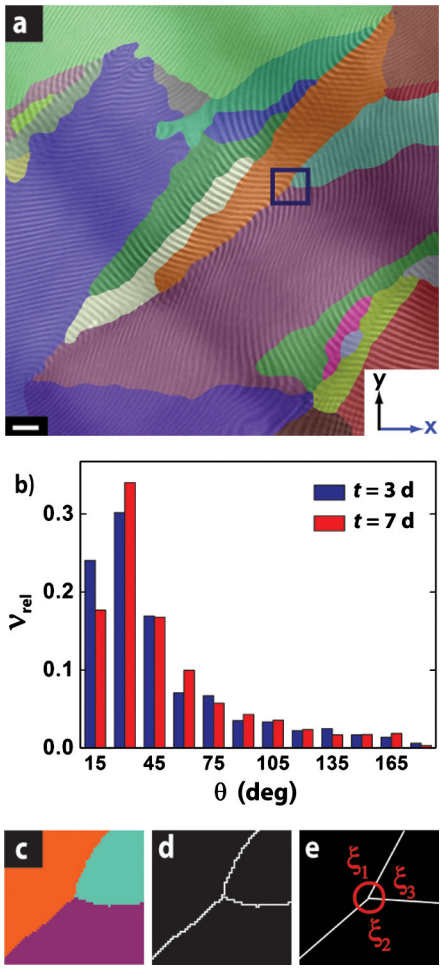

FIG. 2 (color online). Procedure of image and triple-junction analysis. (a) Grain map obtained by image analysis (see text for more details). Scale bar is 200 nm. Encircled area highlights the triple junction that is shown in (c)–(e). (b) Tilt-angle distribution in BCP after 72 h (purple) and 166 h (red) of thermal annealing. (c)–(e) Procedure for triple-junction analysis. Triple-junction (c) after thresholding (d) and subsequently fitting of conic sections to the boundary (e).

and symmetry plane were considered as pure symmetric tilt GBs. Figure 2(b) depicts the tilt-angle distribution of all measured symmetric tilt GBs revealing that the relative GB frequency decreases with increasing tilt angle. The very similar tilt-angle distribution measured after 72 and 166 h of annealing time supports the assumption of local equilibrium in the thermally annealed samples.

In total 408 (744) triple junctions that were analyzed in samples annealed for 72 h (166 h). To determine dihedral angles, conic sections were fitted to the respective boundaries of each triple junction as illustrated in Figs. 2(c)–2(e). Tilt angles θ were binned into $n = 10$ subintervals and GB energies were subsequently determined using the procedure outlined above. Calculated energies were normalized with regard to the maximum energy—errors were estimated by comparison of the calculated results corresponding to 72 and 166 h of thermal annealing. Figure 3(a) depicts the resulting relative energies $E(\theta)$ of symmetric tilt GBs (corresponding to 72 h of thermal annealing) as a function of tilt angle. Because of limitations of the image analysis procedure (in differentiating very low-angle GBs from image artifacts), no data were available for tilt angles $\theta < 5°$, and hence $E(\theta)$ cannot be resolved for angles less than 5°.

Two distinct regimes of the boundary energy can be distinguished in Fig. 3(a) based on their respective dependence on the tilt angle that can be described by the scaling coefficient x of the boundary energy $E(\theta) \sim \theta^x$. In the limit of small tilt angles (here, $5° \leq \theta \leq 10°$), $x \leq 2.5$ is observed, in qualitative agreement with the theoretical limiting value $x = 3$ that has been predicted for small tilt deformations [29]. Since x increases with decreasing θ, we hypothesize that the predicted scaling $E(\theta) \sim \theta^3$ might indeed exist in the vicinity of $\theta = 0$; however, it cannot be resolved by our method due to its limitations in the analysis

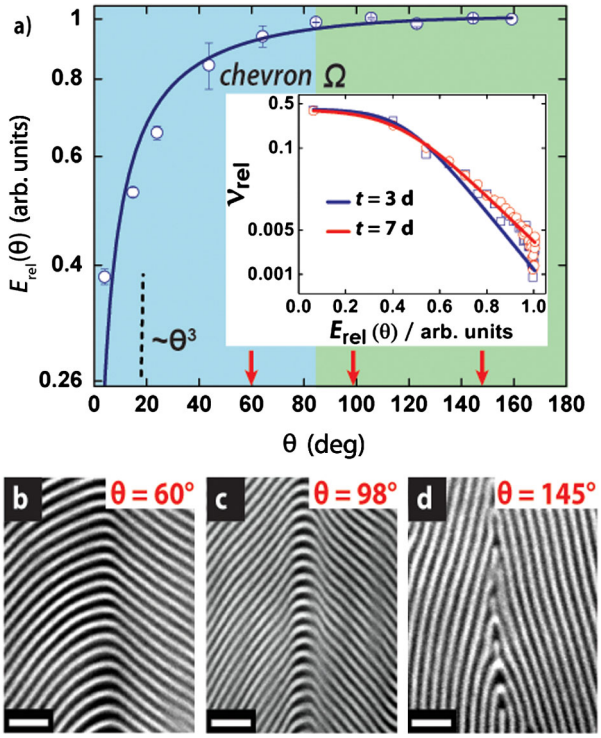

FIG. 3 (color online). Energy map and structure of symmetric tilt boundaries. (a) Plot of the relative GB energy as function of tilt angle after 72 h of thermal annealing (error bars are estimated by the comparison of results at 72 and 166 h of thermal annealing; see text for more details). At the threshold angle $\theta_{crit.} \cong 85°$ a transition from the chevron to the Ω regime is observed. Inset depicts frequency of GB energies—open symbols represent data and continuous lines are introduced to guide the eye. The linear tail in the logarithmic presentation indicates Boltzmann-type distribution of high-angle tilt GBs. Arrows mark angles for which example GB structures are depicted in (b)–(d). (b) Chevron boundary. (c) Intermediate boundary. (d) Ω boundary. Scale bars are 200 nm.

of small tilt-angle boundaries. Note that our results indicate that the θ^3 regime is narrower than predicted by prior simulations—an effect that we interpret as a consequence of the increased degree of segregation [19,20]. A plateau regime is observed for angles exceeding $\theta = \theta_{crit} \cong 85°$, in which the boundary energy is found to be independent (within the experimental error) of the misorientation. In the intermediate tilt-angle range x is found to continuously decrease with increasing misorientation ($2.5 > x \geq 0$). Electron imaging analysis reveals that the onset of the plateau regime ($\theta_{crit} \cong 85°$) is accompanied by the transition of the local structure of symmetric tilt GBs from chevron- [Fig. 3(b)] to Ω-type [Fig. 3(d)] morphologies. This transformation of the local structure of the boundary has indeed been predicted and rationalized with the increased packing frustration of chains within high-angle chevron GBs [18–20]. The chevron $\rightarrow \Omega$ transition was found to occur via a range of intermediate boundary structures [Fig. 3(c)] that are observed around the threshold angle θ_{crit}. As depicted in the inset of Fig. 3(a) the correlation of $E(\theta)$ with the distribution of misorientations [Fig. 2(b)] reveals that the probability of symmetric tilt misorientation between grains decreases with increasing boundary energy. The observed trend is similar to those reported for inorganic polycrystals where experiments and simulations consistently show that the population of grain boundaries is inversely correlated to the grain-boundary energy, but the form of the distribution is not the same in all situations [30,31]. Interestingly, the linear tail of $\log[\nu_{rel}(E(\theta))]$ suggests that distribution of large-angle GB energies is indeed of Boltzmann type (the latter represents the idealized theoretical distribution), whereas for smaller tilt angles a deviation from Boltzmann-type behavior is observed. Deviations from Boltzmann-type distributions have been widely observed in inorganic materials and have been related, for example, to constraints on GB formation implied by the boundary network [31]. We hypothesize that additional contributing factors to non-Boltzmann characteristics could relate to the preferred annealing of low-angle tilt GBs that renders the frequency of low-angle tilt GBs a more complex function of both kinetic and thermodynamic parameters [32]. The coarsening characteristics and GB annealing mechanisms of lamellar BCPs will be discussed in detail in a subsequent publication.

In conclusion, we have presented a methodology for the mapping of GB energies in BCP structures by analysis of triple-junction geometries. For the particular case of symmetric tilt GBs in a strongly segregated lamellar BCP, the results confirm the major predictions of prior simulation studies. Two regimes are observed that correspond to a pronounced increase of boundary energies with increasing tilt angle [the chevron regime with $E(\theta) \sim \theta^x$, $2.5 \geq x \geq 0$] as well as a plateau regime for misorientations exceeding a threshold tilt angle [the Ω regime with $E(\theta) \sim \theta^0$]. The inverse relation between GB energy and frequency of grain misorientation suggests that GB energy is a relevant parameter for grain coarsening of BCP microstructures during thermal annealing. It also highlights unifying characteristics of GB formation in BCPs and inorganic polycrystalline metals and ceramics for which similar relationships have been observed [33]. Because it is known that GB energy is the governing parameter for microstructure formation in inorganic materials, the approach presented here should contribute to a better understanding of microstructural evolution in BCP-based materials that are fundamental to a wide range of novel material technologies.

This work was primarily supported by the National Science Foundation via Grants No. DMR-0706265, No. DMR-1006473, No. EEC-0836633, as well as No. DMR-0804770. H. J. R. acknowledges supplemental Bertucci Graduate Fellowship support. Furthermore, the authors thank the members of the Mesoscale Interphase Mapping Project (MIMP) at Carnegie Mellon for helpful discussions.

*bockstaller@cmu.edu

[1] S. C. Warren, L. C. Messina, L. S. Slaughter, M. Kamperman, Q. Zhou, S. M. Gruner, F. J. DiSalvo, and U. Wiesner, Science **320**, 1748 (2008).
[2] C. Park, J. Yoon, and E. L. Thomas, Polymer **44**, 6725 (2003).
[3] Y. Kang, J. J. Walish, T. Gorishnyy, and E. L. Thomas, Nature Mater. **6**, 957 (2007).
[4] M. R. Bockstaller, R. A. Mickiewicz, and E. L. Thomas, Adv. Mater. **17**, 1331 (2005).
[5] M. R. Bockstaller and E. L. Thomas, Phys. Rev. Lett. **93**, 166106 (2004).
[6] S. P. Gido, J. Gunther, E. L. Thomas, and D. Hoffman, Macromolecules **26**, 4506 (1993).
[7] S. P. Gido and E. L. Thomas, Macromolecules **27**, 849 (1994).
[8] S. P. Gido and E. L. Thomas, Macromolecules **27**, 6137 (1994).
[9] S. P. Gido and E. L. Thomas, Macromolecules **30**, 3739 (1997).
[10] E. Burgaz and S. P. Gido, Macromolecules **33**, 8739 (2000).
[11] J. Listak and M. R. Bockstaller, Macromolecules **39**, 5820 (2006).
[12] L. Qiao and K. I. Winey, Macromolecules **33**, 851 (2000).
[13] D. J. Kinning, E. L. Thomas, and J. M. Ottino, Macromolecules **20**, 1129 (1987).
[14] R. Thompson, J. Chem. Phys. **133**, 144902 (2010).
[15] K. A. Koppi, M. Tirrell, F. S. Bates, K. Almdal, and R. H. Colby, J. Phys. II (France) **2**, 1941 (1992).
[16] K. I. Winey, S. S. Patel, R. G. Larson, and H. Watanabe, Macromolecules **26**, 2542 (1993).
[17] D. L. Polis, S. D. Smith, N. J. Terrill, A. J. Ryan, D. C. Morse, and K. I. Winey, Macromolecules **32**, 4668 (1999).

[18] R. R. Netz, D. Andelman, and M. Schick, Phys. Rev. Lett. **79**, 1058 (1997).
[19] Y. Tsori, D. Andelman, and M. Schick, Phys. Rev. E **61**, 2848 (2000).
[20] M. W. Matsen, J. Chem. Phys. **107**, 8110 (1997).
[21] Note that the intersection of more than three grain boundaries along a line would be energetically unstable. See Ref. [22].
[22] C. S. Smith, *Metal Interfaces* (ASM, Cleveland, 1952), p. 65.
[23] C. Herring, *The Physics of Powder Metallurgy* (McGraw-Hill, New York, 1951), p. 143.
[24] In the case of symmetric tilt grain boundaries in lamellar systems the contributions of torque should vanish due to the symmetry of the boundary. Conversely, torque terms might become relevant for asymmetric GBs or in the case of nonlamellar structures.
[25] B. L. Adams *et al.*, Interface Sci. **7**, 321 (1999).
[26] G. S. Rohrer, J. Mater. Sci. **46**, 5881 (2011).
[27] We note that the condition of local equilibrium is important for the reliable application of the triple-junction technique. Thermal annealing was found to be essential to guarantee local equilibrium in the present study.
[28] The grain identification process was as follows. First, electron micrographs were converted to binary image format. This process removes unnecessary information (such as contrast variation resulting from, for example, knife marks) from the micrographs, but preserves morphological features such as orientation or repeat distance. Subsequently, images were skeletonized to convert the binary domain structures into morphologically equivalent line patterns in which lines delineate domain edge positions. Discrete Fourier transform analysis was applied to the discretized line patterns (30×30 pixel grid size) to determine the orientation of lamellar normals at each grid point with respect to the reference frame [a Cartesian laboratory reference frame was defined such that the film orientation is along the (x, z) plane and the y direction is normal to the film orientation]. Grain maps (as shown in Fig. 2) were constructed by identification of grid points that separate adjacent areas with a difference in orientation of lamellar normal in excess of 15°. For the analysis of low-angle grain boundaries the process was refined accordingly.
[29] P. G. De Gennes and J. Prost, *The Physics of Liquid Crystals* (Oxford University Press, Oxford, 1993), p. 484.
[30] S. J. Dillon and G. S. Rohrer, Acta Mater. **57**, 1 (2009).
[31] G. S. Rohrer, J. Am. Ceram. Soc. **94**, 633 (2011).
[32] Note that the pronounced increase of $E(\theta)$ with θ should render the conversion of high- into low-angle boundaries energetically favorable in the low- and intermediate-angle regime.
[33] D. M. Saylor, A. Morawiec, and G. S. Rohrer, Acta Mater. **51**, 3675 (2003).